

## Search for Invisible Decays of Sub-GeV Dark Photons in Missing-Energy Events at the CERN SPS

D. Banerjee,<sup>11</sup> V. Burtsev,<sup>9</sup> D. Cooke,<sup>11</sup> P. Crivelli,<sup>11</sup> E. Depero,<sup>11</sup> A. V. Dermenev,<sup>4</sup> S. V. Donskov,<sup>8</sup> F. Dubinin,<sup>5</sup> R. R. Dusaev,<sup>9</sup> S. Emmenegger,<sup>11</sup> A. Fabich,<sup>3</sup> V. N. Frolov,<sup>2</sup> A. Gardikiotis,<sup>7</sup> S. N. Gninenko,<sup>4,†</sup> M. Hösken,<sup>1</sup> V. A. Kachanov,<sup>8</sup> A. E. Karneyeu,<sup>4</sup> B. Ketzer,<sup>1</sup> D. V. Kirpichnikov,<sup>4</sup> M. M. Kirsanov,<sup>4</sup> S. G. Kovalenko,<sup>10</sup> V. A. Kramarenko,<sup>6</sup> L. V. Kravchuk,<sup>4</sup> N. V. Krasnikov,<sup>4</sup> S. V. Kuleshov,<sup>10</sup> V. E. Lyubovitskij,<sup>9</sup> V. Lysan,<sup>2</sup> V. A. Matveev,<sup>2</sup> Yu. V. Mikhailov,<sup>8</sup> V. V. Myalkovskiy,<sup>2</sup> V. D. Peshekhonov,<sup>2,\*</sup> D. V. Peshekhonov,<sup>2</sup> O. Petuhov,<sup>4</sup> V. A. Polyakov,<sup>8</sup> B. Radics,<sup>11</sup> A. Rubbia,<sup>11</sup> V. D. Samoylenko,<sup>8</sup> V. O. Tikhomirov,<sup>5</sup> D. A. Tlisov,<sup>4</sup> A. N. Toropin,<sup>4</sup> A. Yu. Trifonov,<sup>9</sup> B. Vasilishin,<sup>9</sup> G. Vazquez Arenas,<sup>10</sup> P. Ulloa,<sup>10</sup> K. Zhukov,<sup>5</sup> and K. Zioutas<sup>7</sup>

(NA64 Collaboration)

<sup>1</sup>Universität Bonn, Helmholtz-Institut für Strahlen-und Kernphysik, 53115 Bonn, Germany

<sup>2</sup>Joint Institute for Nuclear Research, 141980 Dubna, Russia

<sup>3</sup>CERN, European Organization for Nuclear Research, CH-1211 Geneva, Switzerland

<sup>4</sup>Institute for Nuclear Research, 117312 Moscow, Russia

<sup>5</sup>P.N. Lebedev Physics Institute, Moscow, Russia, 119991 Moscow, Russia

<sup>6</sup>Skobel'syn Institute of Nuclear Physics, Lomonosov Moscow State University, 119991 Moscow, Russia

<sup>7</sup>Physics Department, University of Patras, 26504 Patras, Greece

<sup>8</sup>State Scientific Center of the Russian Federation Institute for High Energy Physics of National Research Center 'Kurchatov Institute' (IHEP), 142281 Protvino, Russia

<sup>9</sup>Tomsk Polytechnic University, 634050 Tomsk, Russia

<sup>10</sup>Universidad Técnica Federico Santa María, 2390123 Valparaíso, Chile

<sup>11</sup>ETH Zürich, Institute for Particle Physics, CH-8093 Zürich, Switzerland

(Received 17 October 2016; published 5 January 2017)

We report on a direct search for sub-GeV dark photons ( $A'$ ), which might be produced in the reaction  $e^-Z \rightarrow e^-ZA'$  via kinetic mixing with photons by 100 GeV electrons incident on an active target in the NA64 experiment at the CERN SPS. The dark photons would decay invisibly into dark matter particles resulting in events with large missing energy. No evidence for such decays was found with  $2.75 \times 10^9$  electrons on target. We set new limits on the  $\gamma - A'$  mixing strength and exclude the invisible  $A'$  with a mass  $\lesssim 100$  MeV as an explanation of the muon  $g_\mu - 2$  anomaly.

DOI: 10.1103/PhysRevLett.118.011802

Despite the intensive searches at the LHC and in non-accelerator experiments, dark matter (DM) still is a great puzzle. Though stringent constraints obtained on DM coupling to standard model (SM) particles ruled out many DM models, little is known about the origin and dynamics of the dark sector itself. One difficulty so far is that DM can be probed only through its gravitational interaction. An exciting possibility is that in addition to gravity, a new force between the dark sector and visible matter transmitted by a new vector boson  $A'$  (dark photon) might exist. Such  $A'$  could have a mass  $m_{A'} \lesssim 1$  GeV—associated with a

spontaneously broken gauged  $U(1)_D$  symmetry—and couple to the SM through kinetic mixing with the ordinary photon,  $-\frac{1}{2}\epsilon F_{\mu\nu}A'^{\mu\nu}$ , parametrized by the mixing strength  $\epsilon \ll 1$  [1–3]. This has motivated a worldwide theoretical and experimental effort towards dark forces and other portals between the visible and dark sectors; see Refs. [4,5] for a review. Various theoretical and phenomenological aspects of light vector bosons weakly coupled to quarks and leptons have been also studied in pioneer papers by Fayet [6].

An additional motivation for existence of the  $A'$  has been provided by hints on astrophysical signals of dark matter [7], as well as the  $3.6\sigma$  deviation from the SM prediction of the muon anomalous magnetic moment  $g_\mu - 2$  [8], which can be explained by a sub-GeV  $A'$  with the coupling  $\epsilon \approx 10^{-3}$  [9–11]. Such small values of  $\epsilon$  could naturally be obtained from loop effects of particles charged under both the dark and SM  $U(1)$  interactions with a typical 1-loop

Published by the American Physical Society under the terms of the Creative Commons Attribution 4.0 International license. Further distribution of this work must maintain attribution to the author(s) and the published article's title, journal citation, and DOI.

value  $\epsilon = eg_D/16\pi^2$  [3], where  $g_D$  is the coupling constant of the  $U(1)_D$  gauge interactions.

If the  $A'$  is the lightest state in the dark sector, then it would decay mainly visibly, i.e., typically to SM leptons  $l = e, \mu$  or hadrons, which could be used to detect it. Previous beam dump [12–27], fixed target [28–30], collider [31–33], and rare meson decay [34–43] experiments have already put stringent constraints on the mass  $m_{A'}$  and  $\epsilon$  of such dark photons excluding, in particular, the parameter region favored by the  $g_\mu - 2$  anomaly. However, in the presence of light dark states, in particular dark matter, with the masses  $< m_{A'}$ , the  $A'$  would predominantly decay invisibly into those particles provided that  $g_D > \epsilon e$ . Models introducing such invisible  $A'$  offer new intriguing possibilities to explain the  $g_\mu - 2$  and various other anomalies [44] and are subject to different experimental constraints [45–48]. The most severe limits on the invisible sub-GeV  $A'$  decays have been obtained from the results of beam dump experiments LSND [49,50] and E137 [51], under assumptions on the certain values of the coupling strength  $g_D$  and masses of the DM decay particles. In this Letter we report the first results from the experiment NA64 specifically designed for a direct search of the  $A' \rightarrow$  invisible decay at the CERN SPS.

The method of the search is as follows [52,53]. If the  $A'$  exists it could be produced via the kinetic mixing with bremsstrahlung photons in the reaction of high-energy electrons scattering off nuclei of an active target of a Hermetic detector, followed by the prompt  $A' \rightarrow$  invisible decay into dark matter particles ( $\chi$ ):

$$e^- Z \rightarrow e^- Z A'; \quad A' \rightarrow \text{invisible}. \quad (1)$$

A fraction  $f$  of the primary beam energy  $E_{A'} = fE_0$  is carried away by  $\chi$ 's which penetrate the detector without interactions resulting in an event with zero-energy deposition. While the remaining part  $E_e = (1-f)E_0$  is deposited in the target by the scattered electron. Thus, the occurrence of  $A'$  produced in the reaction (1) would appear

as an excess of events whose signature is a single electromagnetic (EM) shower in the target with energy  $E_e$  accompanied by a significant missing energy  $E_{\text{miss}} = E_{A'} = E_0 - E_e$  above those expected from backgrounds. Here we assume that the  $\chi$ s have to traverse the detector without decaying visibly in order to give a missing energy signature. No other assumptions on the nature of the  $A' \rightarrow$  invisible decay are made.

The NA64 detector is schematically shown in Fig. 1. The experiment employed the optimized 100 GeV electron beam from the H4 beam line. The beam has a maximal intensity  $\approx 4 \times 10^6$  per SPS spill of 4.8 s produced by the primary 400 GeV proton beam with an intensity of few  $10^{12}$  protons on target. The detector utilized the beam defining scintillator (Sc) counters S1 – S3 and veto V1, and magnetic spectrometer consisting of two successive dipole magnets with the integral magnetic field of  $\approx 7$  Tm and a low-material-budget tracker. The tracker was a set of two upstream Micromegas chambers (T1, T2) and two downstream GEM stations (T3, T4) allowing the measurements of  $e^-$  momenta with the precision  $\delta p/p \approx 1\%$  [54]. The magnets also served as an effective filter rejecting the low energy component of the beam. To enhance the electron identification the synchrotron radiation (SR) emitted by electrons was used for their efficient tagging. A 15 m long vacuum vessel between the magnets and the ECAL was installed to minimize absorption of the SR photons detected immediately at the downstream end of the vessel with a SR detector (SRD), which was either an array of  $\text{Bi}_4\text{Ge}_3\text{O}_{12}$  (BGO) crystals or a PbSc sandwich calorimeter of a very fine segmentation [52]. By using the SRD, the initial level of the hadron contamination in the beam  $\pi/e^- \lesssim 10^{-2}$  was further suppressed by a factor  $\approx 10^3$ . The detector was also equipped with an active target, which is an electromagnetic calorimeter (ECAL) for measurement of the electron energy deposition  $E_{\text{ECAL}}$  with the accuracy  $\delta E_{\text{ECAL}}/E_{\text{ECAL}} \approx 0.1/\sqrt{E_{\text{ECAL}}}$ . The ECAL was a matrix of  $6 \times 6$  Shashlik-type modules assembled from Pb and Sc plates with wave length shifting fiber read-out. Each

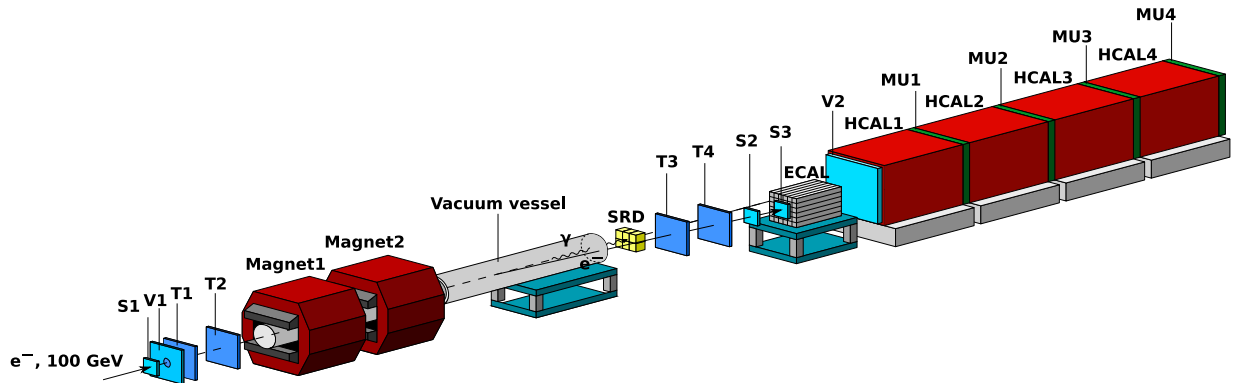


FIG. 1. Schematic illustration of the setup to search for  $A' \rightarrow$  invisible decays of the bremsstrahlung  $A'$ s produced in the reaction  $eZ \rightarrow eZA'$  of 100 GeV  $e^-$  incident on the active ECAL target.

module was  $\approx 40$  radiation lengths. Downstream of the ECAL the detector was equipped with a high-efficiency veto counter V2, and a massive, hermetic hadronic calorimeter (HCAL) of  $\approx 30$  nuclear interaction lengths. The HCAL served as an efficient veto to detect muons or hadronic secondaries produced in the  $e^-A$  interactions in the target. The HCAL energy resolution was  $\delta E_{\text{HCAL}}/E_{\text{HCAL}} \approx 0.6/\sqrt{E_{\text{HCAL}}}$ . Four muon plane counters, MU1-MU4, located between the HCAL modules were used for the muon identification in the final state. The events were collected with the hardware trigger requiring an in-time cluster in the ECAL with the energy  $E_{\text{ECAL}} \lesssim 80$  GeV. The results reported here came mostly from a set of data in which  $n_{\text{EOT}} = 1.88 \times 10^9$  of electrons on target (EOT) were collected with the beam intensity  $\approx 1.4 \times 10^6$   $e^-$  per spill with the PbSc calorimeter. A smaller sample of  $n_{\text{EOT}} = 0.87 \times 10^9$  and an intensity  $I_e = 0.3 \times 10^6$   $e^-$  was also recorded with the BGO detector. Data of these two runs (hereafter called the BGO and PbSc run) were analyzed with similar selection criteria and finally summed up, taking into account the corresponding normalization factors.

In order to avoid biases in the determination of selection criteria for signal events, a blind analysis was performed. Candidate events were requested to have the missing energy in the range  $50 < E_{\text{miss}} < 100$  GeV, which was selected based on the calculations of the energy spectrum of  $A$ 's emitted in the reaction (1) by  $e^\pm$  from the EM shower generated by the beam  $e^-$ s in the target [55]. The HCAL zero-energy threshold was selected to be  $E_{\text{HCAL}} = 1$  GeV, and was determined mostly by the noise of the read-out electronics. Events from a signal box ( $E_{\text{ECAL}} < 50$  GeV;  $E_{\text{HCAL}} < 1$  GeV) were excluded from the analysis of the data until the validity of the background estimate in this

region was established. For the selection criteria optimization, 10% of the data were used, while the full sample was used for the background estimate. The number of signal candidate events were counted after unblinding. A detailed GEANT4 based Monte Carlo (MC) simulation was used to study the detector performance and acceptance, to simulate background sources, and to select cuts and estimate the reconstruction efficiency.

The left panel in Fig. 2 shows the distribution of  $\approx 5 \times 10^4$  events from the reaction  $e^-Z \rightarrow \text{anything}$  in the  $(E_{\text{ECAL}}; E_{\text{HCAL}})$  plane measured with  $2.75 \times 10^9$  EOT. Here,  $E_{\text{HCAL}}$  is the sum of the energy deposited in the first two HCAL modules. Only the presence of a beam  $e^-$  identified with the SR tag was required. Events from the area I in Fig. 2 originate from the QED dimuon production, dominated by the reaction  $e^-Z \rightarrow e^-Z\gamma; \gamma \rightarrow \mu^+\mu^-$  of the muon pair photoproduction by a hard bremsstrahlung photon conversion on a target nucleus and characterized by the energy of  $\approx 10$  GeV deposited by the dimuon pair in the HCAL. This rare process was used as a benchmark allowing us to verify the reliability of the MC simulation, estimate the signal reconstruction efficiency, and cross-check systematic uncertainties. The dimuon production was also used as a reference for the background prediction. The region II shows the SM events from the hadron electroproduction in the target which satisfy the energy conservation  $E_{\text{ECAL}} + E_{\text{HCAL}} \approx 100$  GeV within the energy resolution of the detectors. The leak of these events to the signal box due to the energy resolution was found to be negligible. The events from region III, whose fraction is a few  $10^{-2}$ , are mostly due to pileup of  $e^-$  and beam hadrons.

The candidate events were selected with the criteria chosen to maximize the acceptance for MC signal events and to minimize the numbers of background events,

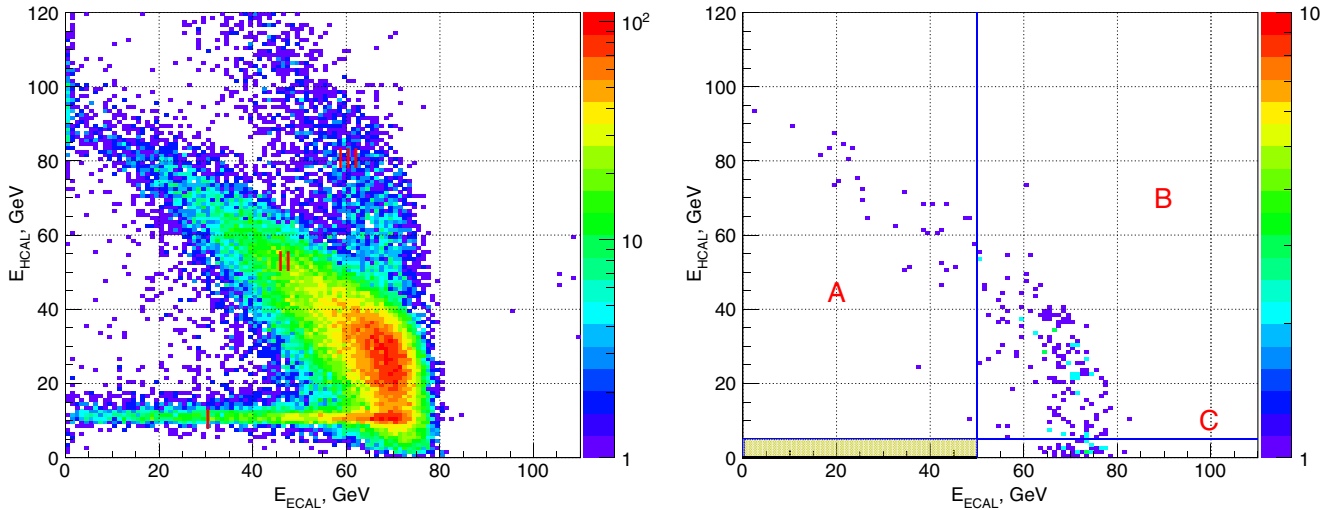


FIG. 2. The left panel shows the measured distribution of events in the  $(E_{\text{ECAL}}; E_{\text{HCAL}})$  plane from the combined BGO and PbSc run data at the earlier phase of the analysis. Another plot shows the same distribution after applying all selection criteria. The dashed area is the signal box region which is open. The side bands A and C are the ones used for the background estimate inside the signal box. For illustration purposes the size of the signal box along the  $E_{\text{HCAL}}$  axis is increased by a factor of 5.

respectively. The following quite moderate selection criteria were applied. (i) The incoming particle track should have a small angle with respect to the beam axis to reject large angle tracks from the upstream  $e^-$  interactions. No cuts on reconstructed momentum were used. (ii) The energy deposited in the SRD detector should be within the SR range emitted by  $e^-$ s and in time with the trigger. This was the key cut identifying the pure initial  $e^-$  state. (iii) The lateral and longitudinal shape of the shower in the ECAL should be consistent with the one expected for the signal shower [55]. (iv) There should be no activity in V2. Only  $\approx 300$  events passed these criteria from combined BGO and PbSc runs.

The search for the  $A' \rightarrow$  invisible decays requires particular attention to backgrounds. Every process with a track and a single EM cluster in the ECAL was considered as a potential source of background. There are several sources which may fake the  $A' \rightarrow$  invisible signal, e.g.,  $e^-$  interactions with the beam line materials resulting in  $e^-$  energy loss,  $\mu \rightarrow e\nu\nu$ ,  $\pi/K \rightarrow e\nu$ ,  $K_{e3}$  decays in flight, energy leakage from particle punchthrough in the HCAL, processes due to pileup of two or more particles, and instrumental effects due to energy loss through cracks in the upstream detector coverage. The selection cuts to eliminate these backgrounds have been chosen such that they do not affect the shape of the true  $E_{\text{miss}}$  spectrum.

Two independent methods were used for the background estimation in the signal region. The first method is based on the MC calculations. Because of the small  $A'$  coupling strength, the fraction of reactions (1) is typically  $\lesssim 10^{-9}$  per incoming  $e^-$ . To study the SM distribution and background at this level is very time consuming. Consequently, we have evaluated with MC simulations all known backgrounds to the extent that it is possible. Events from particle interactions or decays in the beam line, pile-up activity created from them, hadron punchthrough from the target and the HCAL were included in the simulation of background events. Small event-number backgrounds such as the decays of the beam  $\mu$ ,  $\pi$ ,  $K$  or  $\mu$  from the reaction of dimuon production were simulated with the full statistics of the data. Large event-number processes, e.g., from  $e^-$  interactions in the target or beam line, punchthrough of secondary hadrons were also studied extensively, although simulated samples with statistics similar to the data were not feasible. To eliminate possible instrumental effects not present in the MC calculations, the uniformity scan of the central part of the ECAL target was performed with  $e^-$  by using  $T3$  and  $T4$ . We also examined the number of events observed in several regions around the signal box, which were statistically consistent with the estimates.

The two largest sources of background are expected from the beam  $\mu$ ,  $\pi$ ,  $K$  decays in flight. In one case, e.g., when a pion passes through the vacuum vessel it could knock electrons off the downstream window, which hit the SRD, creating a fake tag for a 100 GeV  $e^-$ . Then the pion

TABLE I. Expected numbers of background events in the signal box that passed the selection criteria (i)–(iv) estimated for  $2.75 \times 10^9$  EOT.

Source of background	Events
loss of $e^-$ energy due to punchthrough $\gamma$ s	$< 0.001$
loss of hadrons from $e^-Z \rightarrow e^- + \text{hadrons}$	$< 0.01$
loss or $\mu \rightarrow e\nu\nu$ decays	
of muons from $e^-Z \rightarrow e^-Z\gamma$ ; $\gamma \rightarrow \mu^+\mu^-$	$< 0.01$
$e^-$ interactions in the beam line materials	0.03
$\mu \rightarrow e\nu\nu$ , $\pi/K \rightarrow e\nu$ , $K_{e3}$ decays	0.03
pileup of low energy $e^-$ and $\mu$ , $\pi$ , $K$	
followed by their decays	0.05
$\mu$ , $\pi$ , $K$ interactions in the target	0.02
Total	0.15

could decay into  $e\nu$  in the upstream ECAL region, thus producing the fake signal. Similar background is caused by the pile up of an electron from the low-energy beam tail ( $\lesssim 60$ – $80$  GeV) and a beam  $\mu$ ,  $\pi$ , or  $K$ . The electron could emit the amount of SR energy above the threshold which is detected in the SRD as a tag of 100 GeV  $e^-$  and then is deflected by the magnets out of the detector's acceptance angle. While the accompanied muon or hadron could then decay in flight. For both sources the dominant background came from the  $K_{e3}$  decays. The mistakenly tagged  $\mu$ , and  $\pi$  and  $K$  could also interact in the target producing an EM-like cluster below 50 GeV though the  $\mu Z \rightarrow \mu Z\gamma$  or  $\pi$ ,  $K$  charge-exchange reactions, accompanied by the poorly detected scattered  $\mu$ , or secondary hadrons, respectively. Another background is due to  $e^-$  interactions in the beam line. Table I summarizes the conservatively estimated background inside the signal box, which is expected to be  $0.15 \pm 0.03(\text{stat}) \pm 0.06(\text{syst})$  events. The systematic error includes the uncertainties in the amount of passive material for  $e^-$  interactions, and in the cross sections of the  $\pi$ ,  $K$  charge-exchange reactions on lead (30%).

The second method used the background estimate extracted from the data themselves. MC signal events and the background extrapolated from sidebands A and C shown in the right panel of Fig. 2 were used. Events in the region A ( $E_{\text{ECAL}} < 50$  GeV;  $E_{\text{HCAL}} > 1$  GeV) are pure neutral hadronic secondaries produced by electrons in the ECAL target, while events from the region C ( $E_{\text{ECAL}} > 50$  GeV;  $E_{\text{HCAL}} < 1$  GeV) are likely from the  $e^-$  interactions in the downstream part of the beam line accompanied by bremsstrahlung photons absorbed in the HCAL. The yield of the background events was estimated by extrapolating the observed events to the signal region assessing the systematic uncertainties by varying the background fit functions. Possible variation of the HCAL zero-energy threshold during data taking were also taken into account. Using this, we obtained a second background estimate of  $0.4 \pm 0.3$  events. The background estimates with the two methods are in agreement with each other within errors. After determining all the selection criteria



and estimating background levels, we examined the events in the signal box and found no candidates, as shown in Fig. 2. The conclusion that the background is small is confirmed by the data.

The  $m_{A'}$ -dependent upper limit on the mixing  $\epsilon$  is calculated as follows. For a given number  $n_{\text{EOT}}$  and the mass  $m_{A'}$ , the number of signal events  $N_{A'}$  expected from the reaction (1) in the signal box is given by

$$N_{A'} = n_{\text{EOT}} n_{A'}(\epsilon, m_{A'}, \Delta E_{A'}) \epsilon_{A'}(m_{A'}, \Delta E_{A'}), \quad (2)$$

where  $n_{A'}(\epsilon, m_{A'}, \Delta E_{A'})$  is the yield of  $A'$ 's with the coupling  $\epsilon$ , mass  $m_{A'}$ , and energy in the range  $\Delta E_{A'}$ ,  $0.5E_0 < E_{A'} < E_0$ , per EM shower generated by a single 100 GeV electron in the ECAL [55]. These events correspond to the missing energy  $0.5E_0 < E_{\text{miss}} < E_0$ . The overall signal efficiency  $\epsilon_{A'}$  is slightly  $m_{A'}$ ,  $E_{A'}$  dependent and is given by the product of efficiencies accounting for the NA64 geometrical acceptance (0.97), the analysis efficiency ( $\approx 0.8$ ), veto V2 (0.96), and HCAL signal efficiency (0.94) and the acceptance loss due to pileup ( $\approx 8\%$  for BGO and  $\approx 7\%$  for PbSc runs). The number of collected  $n_{\text{EOT}} = 2.75 \times 10^9$  EOT was obtained from the recorded number of reference events from the EM  $e^-Z$  interactions in the target by taking into account the trigger suppression factor ( $\gtrsim 10^2$ ) and dead time (0.93). The  $e^-$  beam loss due to interactions with the beam line materials was found to be small. The trigger (SRD) efficiency obtained by using unbiased random samples of events that bypass selection criteria was found to be 0.95 (0.97) with a small uncertainty 2% (2%). The  $A'$  acceptance was evaluated by taking into account the selection efficiency for the lateral and longitudinal shape of EM showers in the ECAL from signal events [55]. The  $A'$  yield calculated as described in Ref. [55] was cross-checked with calculations of Ref. [56]. The  $\approx 10\%$  discrepancy between these two calculations was accounted for as systematic uncertainty in  $n_{A'}(\epsilon, m_{A'}, \Delta E_{A'})$  due to a possible difference in treatment of the EM shower development. To estimate additional uncertainty in the  $A'$  yield prediction, the cross-check between a clean sample of  $\approx 5 \times 10^3$  observed and MC predicted  $\mu^+\mu^-$  events with  $E_{\text{ECAL}} \lesssim 60$  GeV was made, resulting in  $\approx 15\%$  difference in the dimuon yield. The number of  $A'$  and dimuon events are both proportional to the square of the Pb nuclear form factor  $F(q^2)$  and are sensitive to its shape. As the mass ( $m_{A'} \approx m_\mu$ ) and  $q^2$  ( $q \approx m_{A'}/E_{A'} \approx m_\mu/E_\mu$ ) ranges for both reactions are similar, the observed difference can be interpreted as due to the accuracy of the dimuon yield calculation for heavy nuclei and, thus, can be conservatively accounted for as additional systematic uncertainty in  $n_{A'}(\epsilon, m_{A'}, \Delta E_{A'})$ . The V2 and HCAL signal efficiency was defined as a fraction of events below the corresponding zero-energy thresholds. The shape of the energy distributions in these detectors from the leak of the signal shower energy in the ECAL was simulated for

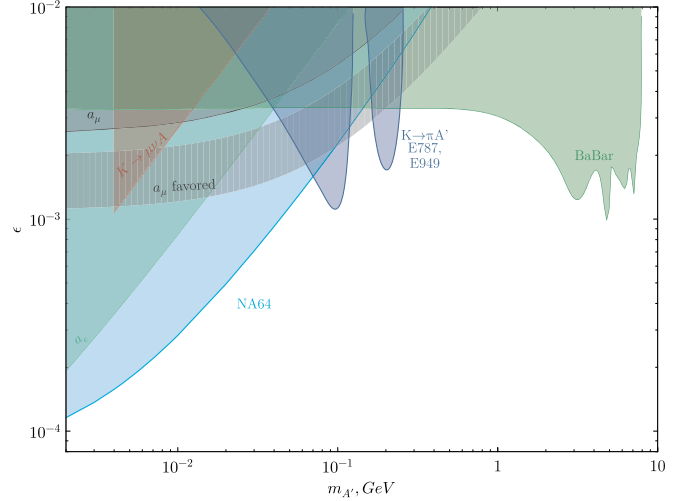


FIG. 3. The NA64 90% C.L. exclusion region in the  $(m_{A'}, \epsilon)$  plane. Constraints from the BABAR [48,56], and E787 + E949 experiments [47,58], as well as the muon  $a_\mu$  favored area are also shown. Here,  $a_\mu = (g_\mu - 2)/2$ . For more limits obtained from indirect searches and planned measurements see, e.g., Ref. [5].

different  $A'$  masses [55] and cross-checked with measurements at the  $e^-$  beam. The uncertainty in the V2 and HCAL efficiency for the signal events, dominated mostly by the pile-up effect from penetrating hadrons in the high intensity PbSc run, was estimated to be  $\approx 3\%$ . Finally, the dominant source of systematic uncertainties on the expected number of signal events comes from the uncertainty in the estimate of the yield  $n_{A'}(\epsilon, m_{A'}, \Delta E_{A'})$  (19%). The overall signal efficiency  $\epsilon_{A'}$  varied from  $0.69 \pm 0.09$  to  $0.55 \pm 0.07$  decreasing for the higher  $A'$  masses.

In accordance with the  $CL_s$  method [57], for zero observed events the 90% C.L. upper limit for the number of signal events is  $N_{A'}^{90\%}(m_{A'}) = 2.3$ . Taking this and Eq. (2) into account and using the relation  $N_{A'}(m_{A'}) < N_{A'}^{90\%}(m_{A'})$  results in the 90% C.L. exclusion area in the  $(m_{A'}, \epsilon)$  plane shown in Fig. 3. These results exclude the invisible  $A'$  as an explanation of the muon  $g_\mu - 2$  anomaly for the masses  $m_{A'} \lesssim 100$  MeV. The further improvement in sensitivity on  $\epsilon$  for the background-free case scales as  $1/\sqrt{n_{\text{EOT}}}$ . Moreover, the results obtained also allow us to restrict other models with light scalars interacting with electrons and decaying predominantly to invisible modes.

We gratefully acknowledge the support of the CERN management and staff and the technical staffs of the participating institutions for their vital contributions. This work was supported by the Helmholtz-Institut für Strahlen- und Kernphysik of the Rheinische Friedrich-Wilhelms University Bonn, University of Bonn (Germany), Joint Institute for Nuclear Research (Dubna), Ministry of Education and Science, and Russian Academy of Sciences (Russia), Swiss National Foundation Grant No 169133 (Switzerland), and grants Fondo Nacional de Desarrollo

Científico y Tecnológico 1140471 and 1150792, Ring ACT1406 and Basal FB0821 Comisión Nacional de Investigación Científica y Tecnológica (Chile). Part of the work on MC simulations was supported by the Russian Science Foundation Grant No. 14-12-01430. We thank S. Andreas and A. Ringwald for their contribution at the earlier stage of the project, and V. Yu. Karjavin, J. Novy, V. I. Savrin, and I. I. Tkachev for their help. We thank COMPASS DAQ group and the Institute for Hadronic Structure and Fundamental Symmetries of TU Munich for the technical support.

\*Deceased.

†Corresponding author.

Sergei.Gninenko@cern.ch

- [1] L. B. Okun, Zh. Eksp. Teor. Fiz. **83**, 892 (1982) [Sov. Phys. JETP **56**, 502 (1982)].
- [2] P. Galison and A. Manohar, Phys. Lett. **136B**, 279 (1984).
- [3] B. Holdom, Phys. Lett. **166B**, 196 (1986).
- [4] J. Jaeckel and A. Ringwald, Annu. Rev. Nucl. Part. Sci. **60**, 405 (2010).
- [5] J. Alexander *et al.*, arXiv:1608.08632.
- [6] P. Fayet, Phys. Lett. **95B**, 285 (1980); Nucl. Phys. **B347**, 743 (1980); Phys. Rev. D **70**, 023514 (2004); **74**, 054034 (2006).
- [7] N. Arkani-Hamed, D. P. Finkbeiner, T. R. Slatyer, and N. Weiner, Phys. Rev. D **79**, 015014 (2009).
- [8] G. W. Bennett *et al.* (Muon G-2 Collaboration), Phys. Rev. D **73**, 072003 (2006).
- [9] S. N. Gninenko and N. V. Krasnikov, Phys. Lett. B **513**, 119 (2001).
- [10] P. Fayet, Phys. Rev. D **75**, 115017 (2007).
- [11] M. Pospelov, Phys. Rev. D **80**, 095002 (2009).
- [12] J. D. Bjorken, R. Essig, P. Schuster, and N. Toro, Phys. Rev. D **80**, 075018 (2009).
- [13] F. Bergsma *et al.* (CHARM Collaboration), Phys. Lett. **166B**, 473 (1986).
- [14] A. Konaka *et al.*, Phys. Rev. Lett. **57**, 659 (1986).
- [15] E. M. Riordan *et al.*, Phys. Rev. Lett. **59**, 755 (1987).
- [16] J. D. Bjorken, S. Ecklund, W. R. Nelson, A. Abashian, C. Church, B. Lu, L. W. Mo, T. A. Nunamaker, and P. Rassmann, Phys. Rev. D **38**, 3375 (1988).
- [17] A. Bross, M. Crisler, S. H. Pordes, J. Volk, S. Errede, and J. Wrbanek, Phys. Rev. Lett. **67**, 2942 (1991).
- [18] M. Davier and H. Nguyen Ngoc, Phys. Lett. B **229**, 150 (1989).
- [19] C. Athanassopoulos *et al.* (LSND Collaboration), Phys. Rev. C **58**, 2489 (1998).
- [20] P. Astier *et al.* (NOMAD Collaboration), Phys. Lett. B **506**, 27 (2001).
- [21] S. Adler *et al.* (E787 Collaboration), Phys. Rev. D **70**, 037102 (2004).
- [22] A. V. Artamonov *et al.* (BNL-E949 Collaboration), Phys. Rev. D **79**, 092004 (2009).
- [23] R. Essig, R. Harnik, J. Kaplan, and N. Toro, Phys. Rev. D **82**, 113008 (2010).
- [24] J. Blumlein and J. Brunner, Phys. Lett. B **701**, 155 (2011).
- [25] S. Gninenko, Phys. Lett. B **713**, 244 (2012).
- [26] J. Blumlein and J. Brunner, Phys. Lett. B **731**, 320 (2014).
- [27] S. Andreas, C. Niebuhr, and A. Ringwald, Phys. Rev. D **86**, 095019 (2012).
- [28] S. Abrahamyan *et al.* (APEX Collaboration), Phys. Rev. Lett. **107**, 191804 (2011).
- [29] H. Merkel *et al.*, Phys. Rev. Lett. **112**, 221802 (2014).
- [30] H. Merkel *et al.* (A1 Collaboration), Phys. Rev. Lett. **106**, 251802 (2011).
- [31] B. Aubert *et al.* (BABAR Collaboration), Phys. Rev. Lett. **103**, 081803 (2009).
- [32] D. Curtin *et al.*, Phys. Rev. D **90**, 075004 (2014).
- [33] J. P. Lees *et al.* (BABAR Collaboration), Phys. Rev. Lett. **113**, 201801 (2014).
- [34] G. Bernardi, G. Carugno, J. Chauveau, F. Dicarolo, M. Dris *et al.*, Phys. Lett. B **166**, 479 (1986).
- [35] R. Meijer Drees *et al.* (SINDRUM I Collaboration), Phys. Rev. Lett. **68**, 3845 (1992).
- [36] F. Archilli *et al.* (KLOE-2 Collaboration), Phys. Lett. B **706**, 251 (2012).
- [37] S. N. Gninenko, Phys. Rev. D **85**, 055027 (2012).
- [38] D. Babusci *et al.* (KLOE-2 Collaboration), Phys. Lett. B **720**, 111 (2013).
- [39] P. Adlarson *et al.* (WASA-at-COSY Collaboration), Phys. Lett. B **726**, 187 (2013).
- [40] G. Agakishiev *et al.* (HADES Collaboration), Phys. Lett. B **731**, 265 (2014).
- [41] A. Adare *et al.* (PHENIX Collaboration), Phys. Rev. C **91**, 031901 (2015).
- [42] J. R. Batley *et al.* (NA48/2 Collaboration), Phys. Lett. B **746**, 178 (2015).
- [43] A. Anastasi *et al.* (KLOE-2 Collaboration), Phys. Lett. B **757**, 356 (2016).
- [44] H. S. Lee, Phys. Rev. D **90**, 091702 (2014).
- [45] E. Izaguirre, G. Krnjaic, P. Schuster, and N. Toro, Phys. Rev. D **88**, 114015 (2013).
- [46] M. D. Diamond and P. Schuster, Phys. Rev. Lett. **111**, 221803 (2013).
- [47] H. Davoudiasl, H. S. Lee, and W. J. Marciano, Phys. Rev. D **89**, 095006 (2014).
- [48] B. Aubert *et al.* (BABAR Collaboration), arXiv:0808.0017.
- [49] B. Batell, M. Pospelov, and A. Ritz, Phys. Rev. D **80**, 095024 (2009).
- [50] P. deNiverville, M. Pospelov, and A. Ritz, Phys. Rev. D **84**, 075020 (2011); arXiv:1107.4580, and note added there.
- [51] B. Batell, R. Essig, and Z. Surujon, Phys. Rev. Lett. **113**, 171802 (2014).
- [52] S. N. Gninenko, Phys. Rev. D **89**, 075008 (2014).
- [53] S. Andreas *et al.*, arXiv:1312.3309.
- [54] D. Banerjee, P. Crivelli, and A. Rubbia, Adv. High Energy Phys. **2015**, 105730 (2015).
- [55] S. N. Gninenko, N. V. Krasnikov, M. M. Kirsanov, and D. V. Kirpichnikov, arXiv:1604.08432 [Phys. Rev. D (to be published)].
- [56] E. Izaguirre, G. Krnjaic, P. Schuster, and N. Toro, Phys. Rev. D **91**, 094026 (2015).
- [57] A. L. Read, J. Phys. G **28**, 2693 (2002).
- [58] R. Essig, J. Mardon, M. Papucci, T. Volansky, and Y. M. Zhong, J. High Energy Phys. **11** (2013) 167.